



**Queensland University of Technology**  
Brisbane Australia

This is the author's version of a work that was submitted/accepted for publication in the following source:

[Agoston, Roland](#), [Izake, Emad L.](#), [Sivanesan, Arumugam](#), [Lott, William B.](#), [Sillence, Martin](#), & [Steel, Rohan](#)  
(2016)

Rapid isolation and detection of erythropoietin in blood plasma by magnetic core gold nanoparticles and portable Raman spectroscopy.  
*Nanomedicine: Nanotechnology, Biology and Medicine*, 12(3), pp. 633-641.

This file was downloaded from: <https://eprints.qut.edu.au/91109/>

© Copyright 2015 Elsevier Inc.

This manuscript version is made available under the CC-BY-NC-ND 4.0 license <http://creativecommons.org/licenses/by-nc-nd/4.0/>

**License:** Creative Commons: Attribution-Noncommercial-No Derivative Works 4.0

**Notice:** *Changes introduced as a result of publishing processes such as copy-editing and formatting may not be reflected in this document. For a definitive version of this work, please refer to the published source:*

<https://doi.org/10.1016/j.nano.2015.11.003>

## Accepted Manuscript

Rapid isolation and detection of erythropoietin in blood plasma by magnetic core gold nanoparticles and portable Raman spectroscopy

Roland Agoston, Emad L. Izake, Arumugam Sivanesan, William B. Lott, Martin Sillence, Rohan Steel

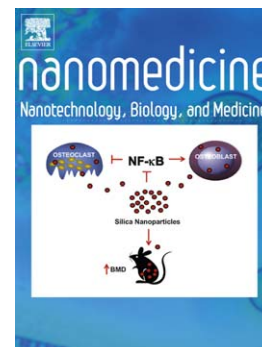
PII: S1549-9634(15)00210-5  
DOI: doi: [10.1016/j.nano.2015.11.003](https://doi.org/10.1016/j.nano.2015.11.003)  
Reference: NANO 1209

To appear in: *Nanomedicine: Nanotechnology, Biology, and Medicine*

Received date: 8 July 2015  
Revised date: 24 September 2015  
Accepted date: 7 November 2015

Please cite this article as: Agoston Roland, Izake Emad L., Sivanesan Arumugam, Lott William B., Sillence Martin, Steel Rohan, Rapid isolation and detection of erythropoietin in blood plasma by magnetic core gold nanoparticles and portable Raman spectroscopy, *Nanomedicine: Nanotechnology, Biology, and Medicine* (2015), doi: [10.1016/j.nano.2015.11.003](https://doi.org/10.1016/j.nano.2015.11.003)

This is a PDF file of an unedited manuscript that has been accepted for publication. As a service to our customers we are providing this early version of the manuscript. The manuscript will undergo copyediting, typesetting, and review of the resulting proof before it is published in its final form. Please note that during the production process errors may be discovered which could affect the content, and all legal disclaimers that apply to the journal pertain.



Rapid isolation and detection of erythropoietin in blood plasma by magnetic core gold nanoparticles and portable Raman spectroscopy

Roland Agoston<sup>a</sup>, Emad L Izake<sup>a\*</sup>, Arumugam Sivanesan<sup>a\*</sup>, William B. Lott<sup>a</sup>, Martin Sillence<sup>a</sup>, Rohan Steel<sup>b</sup>

<sup>a</sup> Nanotechnology and Molecular Sciences Discipline, Faculty of Science and Engineering, Queensland University of Technology, 2 George St., Brisbane, QLD 4001, Australia

<sup>b</sup> Biological Research Unit, Racing Analytical Services Ltd, 400 Epsom Road, Melbourne 3031, VIC, Australia

\*Corresponding author:

E-mail address: e.kiriakous@qut.edu.au (E. L. Izake) Tel.: +61 7 3138 2501; Fax: +61 7 3138 2501

E-mail address: sivanesan.arumugam@qut.edu.au; asnesan@gmail.com (A. Sivanesan) Tel: +61 07 3138 0607

Word count of the abstract= 143

Word count of the manuscript (including body text and figure legends) =4606

Number of references = 60

Number of tables = 1

Number of figures= 7

## Abstract

Isolating, purifying, and identifying proteins in complex biological matrices is often difficult, time consuming, and unreliable. Herein we describe a rapid screening technique for proteins in biological matrices that combines selective protein isolation with direct surface enhanced Raman spectroscopy (SERS) detection. Magnetic core gold nanoparticles were synthesised, characterised, and subsequently functionalized with recombinant human erythropoietin (rHuEPO)-specific antibody. The functionalized nanoparticles were used to capture rHuEPO from horse blood plasma within 15 minutes. The selective binding between the protein and the functionalized nanoparticles was monitored by SERS. The purified protein was then released from the nanoparticles' surface and directly spectroscopically identified on a commercial nanopillar SERS substrate. ELISA independently confirmed the SERS identification and quantified the released rHuEPO. Finally, the direct SERS detection of the extracted protein was successfully demonstrated for in-field screening by a handheld Raman spectrometer within 1 minute sample measurement time.

## Key words

Selective isolation, Label-free SERS, Magnetic core gold nanoparticles, Erythropoietin, In-field screening, Proteins in biological fluids

## Background

The efficient and accurate analysis of biomolecules found in complex biological matrices like blood or urine is essential for many applications, including protein characterization, clinical diagnostics, and drug dosing protein analysis, but current methods are usually expensive and time consuming [1-4]. Simultaneous methods for sample separation and detection must exhibit sufficiently high resolution, high sensitivity and wide dynamic range to detect low concentrations of proteins [5-7]. Ideally, these methods should also be easy to perform, rapid, non-toxic, environment-friendly, and cost-effective. No current protein detection technique meets all these demands [5-7]. Although mass spectrometry (MS) is sensitive and accurate for the analysis of proteins [8, 9], it is relatively expensive, requires specialised skills, and cannot be field adapted.

Enzyme-linked immunosorbent assay (ELISA) is a widely used technique in protein analysis. ELISA methods fall in two categories, direct and indirect. The direct methods use only one primary antibody while the indirect methods use primary and secondary antibodies. Direct ELISA methods have significant disadvantages such as: 1) the antibody's immune-reactivity is adversely affected by labelling with enzymes or tags; 2) labelling the used antibody is time-consuming and expensive; 3) there is only a limited choice of antibody labels that can be used from one experiment to another; 4) the signal amplification is modest. Indirect ELISA methods suffer from other disadvantages such as the long analysis time, due to the introduction of extra incubation steps in the procedure, and cross-reactivity with the secondary antibody, which result in nonspecific signals [10].

Surface-enhanced Raman spectroscopy (SERS), which characterises molecules by their vibrational fingerprint, is a rapidly emerging technique for the detection of biomolecules [11-12]. In SERS, the surface plasmon resonance (SPR) of a nanostructured noble metal surface

enhances the oscillating electric field of incident light [13]. This near-field enhancement increases the Raman signal of analyte molecules that are in close proximity to the metal surface by factors as high as  $10^6$ – $10^8$  relative to the unenhanced Raman signal [13-15], making it useful for ultra-trace detection and potentially allowing for single-molecule detection [16, 17].

SERS strategies may be employed to either directly or indirectly detect biomolecules. In the direct method, a biological sample is loaded onto a noble metal substrate and directly analysed by SERS to acquire the Raman signature of the biomolecule [18-20]. SERS provides direct structural information about the bound target molecule and identifies qualitative differences between similar samples. However, this approach lacks specificity and the Raman spectroscopic features other molecules present in a complex biological matrix can obscure the Raman characteristics of the target analyte. For this reason, extensive isolation and clean-up procedures are required prior to direct SERS detection [21]. By comparison, SERS may indirectly detect biomolecules by attaching a Raman-active dye to the metal SERS substrate [20, 22]. The substrate's surface carrying the Raman dye is then pacified with a protective layer (e.g. silica shell) to prevent the non-specific binding of potentially interfering biomolecules in a complex biological matrix. Analyte-specific recognition molecules, such as antibodies or aptamers, are attached to the SERS substrate to provide target specificity [20]. However, indirect SERS detection does not detect the target biomolecule itself, but only detects the SERS spectrum of the Raman dye [21]. Specific recognition of the target analyte by the antibody or aptamer must be assumed to occur without significant cross reactivity.

We recently demonstrated a hybrid approach for label-free indirect SERS detection of proteins, in which a SERS substrate was functionalized with a protein-specific antibody or aptamer for target specificity, but no Raman dye was attached to the SERS substrate [21, 22].

Instead, the SERS spectra of surface-bound antibody or aptamer were compared before and after the binding of the target protein. Differences in features between the spectra were used to identify the target protein in aqueous and biological samples.

Erythropoietin (EPO) is a glycoprotein hormone used in the regulation of erythropoiesis and is involved as a signalling protein in the production of red blood cells in bone marrow [23]. Sports doping with exogenous rHuEPO increases oxygen capacity and leads to enhanced aerobic performance by athletes. The short biological half-life of rHuEPO makes it only detectable in urine for 3–7 days [24–26]. Recent doping regimens, in which micro-doses of rHuEPO (approximately 20–25 IU/kg) are administered to avoid random detection by anti-doping authorities, have reduced the rHuEPO detection window to only 12–18 hours [27]. The standard protocol currently used to detect rHuEPO doping in competitive sports, isoelectric focusing and double blotting [28], takes several days to perform in a laboratory-based environment and requires skilled technicians, complex procedures, and expensive equipment. To detect rHuEPO doping in sports environment, a reliable rHuEPO screening technique is required that is both rapid and field adaptable. In order to identify rHuEPO in urine and blood, the existing reference techniques attempt direct detection of the substance and/or its metabolite in its original biological matrix [7, 29]. This requires extensive clean-up procedures to isolate the protein from the biological matrix of origin prior to the measurement.

Here we introduce a modified approach for simplified selective isolation and label-free direct SERS detection of rHuEPO to demonstrate the utility of this technique for detecting biomolecules in complex biological matrices. We first developed magnetic core gold nanoparticles and functionalized their surfaces with rHuEPO-specific antibodies to create a rHuEPO-specific recognition layer. The remaining bare gold surface on the nanoparticles

surface was pacified by backfilling with an alkane thiol to block non-specific binding of potentially interfering molecules. The functionalized nanoparticles selectively captured rHuEPO from spiked horse plasma. The binding event between rHuEPO and the functionalized nanoparticles was monitored by SERS [30]. To confirm the selective capture of rHuEPO, as well as to directly detect its Raman fingerprint, the bound rHuEPO molecules were released from the extractor nanoparticles, loaded onto a gold-coated silicon nanopillar substrate and characterised by SERS. To cross-validate our methodology, rHuEPO that had been captured by our functionalized nanoparticles was screened by an independent laboratory using rHuEPO-specific ELISA. Finally, to demonstrate applicability of this new method for the in-field rapid screening of rHuEPO, we directly acquired the SERS spectrum of the captured and released rHuEPO using a handheld Raman device and compared it to a standard rHuEPO SERS spectrum.

The significant advantages of the protein analysis methodology that we describe here include: 1) the rapid and selective isolation of the target proteins directly from a complex biological matrix; 2) the ability to monitor the selective antibody-antigen binding event by SERS; 3) the ability to directly detect the native protein's Raman fingerprint by SERS; and 4) the applicability of this technique to the rapid detection of proteins in the field.

## **Methods**

### *Chemicals and reagents*

Recombinant human erythropoietin international standard (rHuEPO IS, 3<sup>rd</sup> International Reference Preparation) was sourced from the National Institute for Biological Standards and Control, UK. 7D3 mouse monoclonal anti-human erythropoietin antibody was purchased from MAIA Diagnostics, Uppsala, Sweden. Gold (III) chloride (HAuCl<sub>4</sub>), phosphate buffered saline, bovine serum albumin, sodium borohydride (NaBH<sub>4</sub>, 99%), trisodium citrate



( $\text{Na}_3\text{C}_6\text{H}_5\text{O}_7 \cdot 2\text{H}_2\text{O}$ ), ferrous chloride ( $\text{FeCl}_2 \cdot 4\text{H}_2\text{O}$ ), ferric chloride ( $\text{FeCl}_3 \cdot 6\text{H}_2\text{O}$ ), nitric acid and sodium hydroxide were of analytical grade and purchased from Sigma-Aldrich (USA). Gravity flow size-exclusion columns (illustra NAP-5) were obtained from GE Healthcare Life Sciences (AU). Deionized water (ultrapure Millipore filtered,  $18.2 \text{ M}\Omega \cdot \text{cm}@25^\circ\text{C}$ ) was used in all preparations. All glassware was cleaned with aqua regia and thoroughly rinsed with deionized water prior to use. Quantikine IVD human erythropoietin ELISA kit from R&D Systems (USA, catalogue No DEP00) was used for the detection of rHuEPO in horse plasma.

#### *Synthesis of iron oxide nanoparticles*

To develop the magnetic iron oxide cores,  $\text{Fe}_3\text{O}_4$  nanoparticles were first prepared by precipitation, and then chemically oxidized to  $\gamma\text{-Fe}_2\text{O}_3$  [31, 32]. Briefly,  $\text{FeCl}_3 \cdot 6\text{H}_2\text{O}$  (10 mmol) and  $\text{FeCl}_2 \cdot 4\text{H}_2\text{O}$  (5 mmol) were dissolved in dilute hydrochloric acid solution (12.5 mL, 0.36 M) with magnetic stirring. The developed clear yellow solution was then added dropwise to NaOH solution (125 mL, 1.5 M) with vigorous stirring where a black precipitate was immediately formed. The resulting mixture was stirred for 10 minutes after complete addition. The formed precipitate was then collected using strong permanent magnet. To neutralize the pH of the precipitate, it was rinsed with dilute hydrochloric acid solution (250 mL total, 0.01 M). Finally, the precipitate was washed several times with deionized water. The washed precipitate was then re-suspended in dilute nitric acid solution (125 mL, 0.01 M), boiled to reflux for one hour, then cooled to room temperature. The resulting iron oxide nanoparticles were collected using a magnet and rinsed several times with deionized water to neutralize the medium. The clean brown-coloured product was resuspended in 50 mL of deionized water, and the concentration was determined gravimetrically to be 0.177 M.

*Development of magnetic core gold nanoparticles*

To develop a gold shell onto the iron oxide nanoparticle surface, a method described by Tamer et. al [33] was adopted with modifications. 0.6 mL of the iron oxide nanoparticle colloid (0.177 M) was transferred into a 100 mL volumetric flask and diluted with deionized water. 19 mL of the resulting solution was transferred to another round-bottomed flask. HAuCl<sub>4</sub> (0.5 mL, 1%) was then added and the resulting mixture diluted to 100 mL with deionized water. To reduce gold atoms onto the iron oxide nanoparticles' surface, freshly prepared NaBH<sub>4</sub> solution (0.2 mL, 0.05 M) was added to the mixture, followed by 5 successive additions of 0.1 mL NaBH<sub>4</sub> (0.05 M). The mixture was vigorously swirled for 10 minutes after each addition. The mixture was then heated to boil and 3 mL of sodium citrate solution (0.1 M) was added dropwise to produce a pink coloured colloid. The formed magnetic core gold nanoparticles were removed from the reaction mixture using a magnet. The nanoparticles were then washed several times with D.I water and finally resuspended in 4 mL of D.I water.

*Development of antibody-functionalized magnetic core gold nanoparticles*

To attach the 7D3 anti rHuEPO antibodies to the gold surface of the magnetic core gold nanoparticles, cysteamine was used as a linker. The amine group of cysteamine was utilized to form amide bond with the C-terminus of the antibody structure [34]. For this purpose, 1-ethyl-3-(3-dimethylaminopropyl) carbodiimide solution (EDAC, 0.2 M) and N-hydroxysuccinimide solution (NHS, 0.1 M) were prepared in PBS (pH 7.4) and used to activate the -COOH groups of the 7D3 anti-rHuEPO antibody [34]. 50  $\mu$ L of both EDAC and NHS solutions were added to a LoBind vial and vortexed for 15 minutes. 100  $\mu$ L of aqueous cysteamine ( $3 \times 10^{-5}$  M) was then added to the vial and mixed for another 15 minutes. 50  $\mu$ L of

the 7D3 anti-rHuEPO antibody ( $2 \times 10^{-5}$  M in PBS, pH 7.4) was then added to the mixture in ten equal volumes with 2 minutes vortex between additions. After complete mixing, the solution was allowed to stand for 5 hours under dark conditions at 4°C. After this time, the reaction mixture was purified using a gravity flow size-exclusion column to obtain the cysteamine-bound 7D3 antibody.

To attach the cysteamine-bound 7D3 antibody to the magnetic core gold nanoparticles, 100  $\mu$ L of the nanoparticles were mixed with 50  $\mu$ L of the antibody in a LoBind Eppendorf vial and left to form Au-S bonds between the thiol (-SH) group of cysteamine-bound antibodies and the gold surface of the nanoparticles overnight at 4°C. To prevent non-specific binding of interfering analytes and enhance the selectivity of the functionalized nanoparticles towards the target protein, any remaining bare sites (i.e. gold surface areas that were not occupied by the antibodies) were backfilled by adding 15  $\mu$ L of 1-butanethiol ( $1 \times 10^{-6}$  M in PBS, pH 7.4) and allowing the mixture to stand for at 1 hour [35, 36]. The backfilled functionalized magnetic core gold nanoparticles were then separated using a magnet, resuspended in 100  $\mu$ L PBS (pH 7.4), and stored in a refrigerator at 4°C.

#### *Selective isolation and SERS monitoring of rHuEPO binding to functionalized nanoparticles*

The backfilled functionalized nanoparticles were used to selectively capture rHuEPO from aqueous solution. An aqueous standard of rHuEPO ( $1.1 \times 10^{-8}$  M in PBS buffer, pH 7.4) was added to the functionalized nanoparticle colloid in the ratio of 1:10 v/v. The mixture was left to stand for 15 minutes to complete binding between the antibody and rHuEPO. The protein-bearing functionalized nanoparticles were then collected using a magnet and washed several times with PBS buffer (pH 7.4) to remove unbound protein. The protein-bearing functionalized nanoparticles were then screened using SERS and the acquired spectrum

compared to that of the functionalized nanoparticles prior to their interaction with the rHuEPO.

For the isolation of rHuEPO from a biological matrix, rHuEPO spiked horse plasma was mixed with the backfilled functionalized nanoparticles and PBS buffer (pH 7.4) in the ratio of 1: 5: 50 respectively, to a total volume of 100  $\mu$ L. The final concentration of rHuEPO in the mixture was 1 nM. The mixture was then left to stand for 15 minutes to the complete binding between the nanoparticles and rHuEPO. The nanoparticles were then magnetically removed from the matrix and rinsed several times with PBS buffer (pH 7.4) to remove any unbound proteins.

Blank horse plasma samples were donated by Biological Research Unit, Racing Analytical Services Ltd, Melbourne. The samples were collected under the Melbourne lab protocols and ethical clearances, arrangements and protocols are all maintained by this lab. The samples were also shipped under their lab protocols for shipping biological specimens. The samples were received at QUT and used as a matrix for Raman testing.

#### *Direct SERS detection and ELISA assay of extracted rHuEPO from horse plasma*

For the direct SERS detection of rHuEPO from spiked horse plasma, the protein-bearing functionalized nanoparticles were reconstituted in 100  $\mu$ L of N-acetyl glucosamine buffer to release the captured protein [37]. The released protein solution was then loaded onto a preconditioned gravity flow size exclusion column for 5 minutes to remove the buffer. The protein was eluted off the column using 500  $\mu$ L of deionized water. 10  $\mu$ L of the clean rHuEPO solution was then loaded onto gold-coated silicon nanopillars SERS substrate [38, 39] and directly screened by SERS for 1 minute using the Renishaw inVia Raman Microscope as well as a handheld Raman spectrometer (ID Raman, ocean optics, USA).

For cross validation of the SERS measurements, aliquots of the extracted rHuEPO were submitted to independent screening by Solid Phase Sandwich ELISA [40] at the research unit, Racing Analytical Services Ltd, Melbourne, Australia.

#### *Instrumentation and spectroscopic measurements*

The iron oxide nanoparticles and the magnetic core gold nanoparticles were characterised by transmission electron microscopy (TEM) [JEOLJEM-1400 (JEOL, USA)] and UV–visible spectroscopy [Cary 100 spectrophotometer (Agilent Technologies, USA)]. For the determination of the iron oxide phase, samples were dried and prepared as a thin film, then the X-Ray diffraction patterns were collected using a Philips X'pert wide angle X-Ray diffractometer operating in step scan mode, with Co K $\alpha$  radiation (1.7903 Å). Patterns were collected in the range 10 to 80° 2 $\theta$  with a step size of 0.02° and a rate of 30s per step. The XRD patterns were matched with ICSD reference patterns using the software package HighScore Plus.

Raman spectra were collected on the Renishaw inVia Raman Microscope using an excitation wavelength of 785 nm and 0.5% of maximum (450mW) laser power. Spectra were collected by a 50x objective lens over a wavelength range from 300 cm<sup>-1</sup> to 1800 cm<sup>-1</sup> using 10 accumulations (1 second exposure time per accumulation). At least 30 spots, on various locations of the SERS substrate, were screened per each submitted sample.

For SERS measurement using the handheld IDRaman Mini, the sample was screened in the Raster Orbital Scanning (ROS) mode using 785 nm excitation wavelength and 40 accumulations per minute per sample [41].

## Results

### *Synthesis and characterization of magnetic core gold nanoparticles*

The attraction towards magnetic core gold nanoparticle synthesis is due to their novel properties and potential applications in various fields such as cellular hyperthermia [42], magnetic resonance imaging [43], drug and gene delivery [44], as well as biotechnology [45]. In these applications, the iron oxide core performs as a giant paramagnetic atom with a fast response to the applied magnetic field especially when the size of the core is between 5 and 20 nm [46]. Gold is chemically stable, biocompatible, and has excellent plasmonic properties for SERS [47]. Due to the surface chemistry of gold, the development of gold shells onto the iron oxide nanoparticles surface facilitates the functionalization of the nanoparticles with EPO-specific antibody [48] as well as enhances the stability of the magnetic core of the nanoparticles [31-32].

In this work,  $\gamma$ -Fe<sub>2</sub>O<sub>3</sub> nanoparticles were synthesised for the deposition of a gold shell [51, 52]. The synthesized nanoparticles were spherical in shape with a mean size distribution of 10±2 nm as characterized by TEM (Fig 1a). The phase of the  $\gamma$ -Fe<sub>2</sub>O<sub>3</sub> nanoparticles was confirmed by X-ray diffraction (Fig. 2). Both the magnetite and maghemite phases have the same spinel structure as well as very similar lattice parameters. The peaks at diffraction angles (2 $\theta$ ) of 35.3°, 41.7°, 50.8°, 67.7°, and 74.9° degrees indicate that the pattern could be indexed to a cubic structure of either magnetite or maghemite. The peaks at 24.7° and 21.3° also suggest the presence of both magnetite and maghemite phases of the iron oxide. However, the high intensity of the peak at 41.7 indicates that the iron oxide nanoparticles exist predominantly in the maghemite phase [46].

To develop a gold shell onto the surface of the magnetic nanoparticles, iterative reduction of HAuCl<sub>4</sub> was carried out using sodium borohydride to initially nucleate gold onto the iron

oxide nanoparticles surface. Subsequent sodium citrate reduction of  $\text{Au}^{3+}$  ions to Au expanded the nucleated gold into a shell around the magnetic core. The resulting magnetic core gold nanoparticles were spherical with an average size of  $15\pm 6$  nm as indicated by TEM (Fig.1b). The plasmonic properties of the magnetic core gold nanoparticles were confirmed by a characteristic plasmon band at 530 nm observed by UV–visible spectroscopy (Fig. 3).

#### *Selective isolation and SERS monitoring of rHuEPO binding to magnetic core gold nanoparticles*

The magnetic core gold nanoparticles were then functionalized with 7D3 anti-rHuEPO antibodies and used for the selective isolation of rHuEPO. Functionalizing a gold nanoparticle surface with antibodies has been previously described [34], where cysteamine was used to link an active carboxylic acid terminus, of Aflatoxin B1 antibody (via an amide bond) to the gold surface. Unfortunately, cysteamine on a gold surface may adopt a gauche configuration in which the cysteamine molecule binds to the gold nanoparticles from both its thiol and amine ends [49]. In this conformation, the amine group of cysteamine would not be available to bind the antibody [50]. To maximize the number of antibody molecules bound to the surface of gold nanoparticles and enhance the capacity of the nanoparticles to bind the target protein, the amide bond between cysteamine and the active 7D3 antibody carboxylate groups was formed in solution. Next, the cysteamine-bound antibody was attached to the gold surface of the magnetic core nanoparticles via an Au-S bond. The unfunctionalized areas of the nanoparticles' surface were backfilled with 1-butanethiol to prevent non-specific binding of interfering analytes and ensure the selectivity of the nanoparticles towards rHuEPO.

#### **Discussion**

Once functionalized and blocked, the magnetic core gold nanoparticles were then used to isolate rHuEPO from an aqueous solution. The binding of rHuEPO to the functionalized

nanoparticles was directly monitored by comparing the SERS spectra of the nanoparticles before and after interaction with the protein. The SERS spectrum of the functionalized nanoparticles before interaction with the protein is depicted in figure 4a. The Raman bands at  $565\text{ cm}^{-1}$ ,  $752\text{ cm}^{-1}$  and  $1549\text{ cm}^{-1}$  are characteristic of the antibody tryptophan residues [51-54, 55]. The  $960\text{ cm}^{-1}$  band represents a C-C stretching vibrational mode [51, 54] and the  $1062\text{ cm}^{-1}$  band may be attributed to a C-N stretching vibrational mode [51, 53, 56]. The characteristic band at  $1203\text{ cm}^{-1}$  arose from the phenylalanine and tyrosine residues in the antibody [51, 53, 56]. The  $1425\text{ cm}^{-1}$  band may be attributed to the tyrosine residues and the CH vibrations of tryptophan indole rings within the antibody skeleton [51, 54]. Finally the band at  $1584\text{ cm}^{-1}$  may be attributed to Tryptophan, Tyrosine, Phenylalanine residues [53, 55, 58] while the band at  $1611\text{ cm}^{-1}$  is due to Phenylalanine and amide I ( $\alpha$  helix) vibration modes [51, 52, 57].

The SERS spectrum of the functionalized nanoparticles after interaction with rHuEPO (Fig 4b) showed significant changes in spectral features that may be attributed to the binding event between the 7D3 antibody and the target protein [58]. The characteristic tryptophan Raman bands now appear at  $786\text{ cm}^{-1}$ ,  $871\text{ cm}^{-1}$  and  $1584\text{ cm}^{-1}$  [51]. The band at  $1437\text{ cm}^{-1}$  may be attributed to  $\text{CH}_2$  scissoring vibration mode [51, 54, 55, 57]. The band at  $1028\text{ cm}^{-1}$  may be attributed to the in-plane ring CH deformation of the phenylalanine residues of the protein [51]. The low intensity of this band suggests that the phenyl ring approaches the gold surface of the nanoparticles but is not directly adsorbed onto the surface. Thus, the phenyl ring-nanoparticles interaction is weak [51]. The absence of the phenyl ring breathing vibration at  $1002\text{ cm}^{-1}$  also suggests that the protein is not directly adsorbed onto the gold nanoparticles and the rHuEPO phenylalanine residues reside at a distance from the substrate's gold surface [51].



The asymmetric vibrations ( $C\alpha$  CN and  $NH_3^+$  deformation) of the  $CNH_2$  groups within the protein structure are expressed by the band at  $1132\text{ cm}^{-1}$  [51, 53, 55, 56]. The amide III vibrations of the complex formed between the antibody and rHuEPO are indicated by two Raman bands at  $1225\text{ cm}^{-1}$  and  $1248\text{ cm}^{-1}$  [51, 52, 55, 57]. The weak band at  $1523\text{ cm}^{-1}$  may be attributed to the amide II vibration of antibody-rHuEPO complex [51, 53]. Despite the fact that the amide II band of proteins is Raman inactive, it may become enhanced when the protein structure is immobilized in a close proximity to the surface of a noble metal [51]. Finally, the amide I vibration of the antibody-EPO complex now appears at  $1642\text{ cm}^{-1}$  [51-54, 55, 57]. The spectral differences between the free functionalized nanoparticles and the rHuEPO-bound nanoparticles were used to monitor the binding event between the protein and the functionalized nanoparticles and, in effect, the selective isolation of the target protein from the sample matrix. This process is simple and does not require complex pretreatment and preconcentration procedures as in the case of other techniques, such as HPLC-MS.

#### *Direct SERS detection of rHuEPO*

To confirm the selective isolation of rHuEPO and to demonstrate the direct detection of the extracted protein by SERS, we used the functionalized nanoparticles to extract the protein from spiked horse plasma. The captured protein was then released from the nanoparticles' surface using a releasing buffer [59]. The purified protein extract was then directly screened by SERS. The SERS spectra of the extracted protein and rHuEPO standard are depicted in figure 5a,b and show significant correlation. The SERS spectrum of the extracted rHuEPO (Fig. 5b) shows the characteristic Raman bands of a protein (Table 1).

For cross-validation purposes, an aliquot of the protein extract was also screened by independent analytical services laboratory using ELISA. The ELISA screening confirmed that rHuEPO was present in the protein extract at concentration of  $72\text{ mIU/mL}$  ( $553.7\text{ pg/mL}$ ).

*Direct SERS detection of rHuEPO by handheld Raman spectrometer*

In order to demonstrate our methodology for the in-field screening of rHuEPO in biological matrices, we loaded the protein extract (from horse plasma) onto a commercial SERS substrate and used a handheld Raman spectrometer for the direct SERS detection of rHuEPO. The SERS spectra of the extracted protein and rHuEPO standard are depicted in figure 6a,b. The match between the two spectra is obvious. The measurements were carried out in the Raster Orbital Scanning (ROS) mode and took only one minute per sample to acquire the SERS spectrum. This sample scanning mode allows for scanning large area of the sample with a tightly focused laser beam. The ability to screen a large area of the sample increases the number of Raman-active molecules being probed by the excitation laser beam and, therefore, provides higher sensitivity data. The quality and the notable match in the SERS spectra (Fig. 6a,b) may be attributed to the ability of the ROS screening mode to acquire an average SERS spectrum from the entire sample load on the SERS substrate [43, 60].

In order to demonstrate the capacity of our protein analysis method, towards SERS quantification of rHuEPO, various concentrations of in the range of 50nM – 5 pM aqueous rHuEPO were employed. To each concentration of rHuEPO, a fresh substrate was used for the SERS quantification by the handheld Raman spectrometer. The laser power at the sample was 50 mW and a 5 second accumulation was carried out for each concentration. The band at  $1551\text{ cm}^{-1}$  was used as a reference band for rHuEPO quantification. The SERS signals were found to decrease with decreasing concentration as indicated by Figure 7a. A linear relationship was obtained between the SERS signal intensity at  $1551\text{ cm}^{-1}$  and the corresponding rHuEPO log concentration plot is depicted in Figure 7b. As indicated by Figure 7b, close correlation ( $r^2 = 0.995$ ) was found over the concentration range of 50 nM to

5 pM rHuEPO. The minimum limit of detection was estimated mathematically using the regression equation in figure 7b and found to be 1 pM.

In conclusion, we demonstrated the selective isolation and direct SERS detection of rHuEPO using antibody-functionalized nanoparticles and SERS. The changes in the SERS spectrum of the antibody-functionalized nanoparticles after their binding to a protein allow for monitoring the binding event by SERS. The direct SERS detection of extracted rHuEPO from a biological matrix is demonstrated for the first time. The SERS detection of the protein was supported by ELISA, which confirmed and quantified the rHuEPO in the protein extract. The iron core of the gold-coated nanoparticle plays a key role in the magnetically induced separation of rHuEPO from the matrix. However it does not play any operational role in the detection process of rHuEPO. The burden of detection rests entirely on the plasmonic response of the Au shell and thus the detection mechanism is independent of whether the core is magnetic or not. Finally, the methodology was successfully utilized for the rapid in-field screening of rHuEPO within a biological matrix using a commercial SERS substrate and handheld Raman device. This study demonstrates a proof of concept for the combined selective isolation and in-field direct SERS detection of proteins in complex matrices. Our future work is directed towards reproducible direct SERS quantification of ultra-trace amounts of proteins in biological matrices using the demonstrated methodology and handheld spectrometer.

**References**

- [1] Finoulst I, Pinkse M, Van Dongen W, Verhaert P. Sample preparation techniques for the untargeted LC-MS-based discovery of peptides in complex biological matrices. *J Biomed Biotechnol* 2011; DOI: 10.1155/2011/245291
- [2] Poliwoda A, Wieczorek P. P. Sample pretreatment techniques for oligopeptide analysis from natural sources. *Anal Bioanal Chem* 2009; **393**: 885-897
- [3] Miękus N, Olędzka I, Plenis A, Woźniak Z, Lewczuk A, Koszałka P, Seroczyńska B, Bączek T. Gel electrophoretic separation of proteins from cultured neuroendocrine tumor cell lines. *Mol Med Rep*, 2015; **11**: 1407-1415
- [4] Mirzaei H, Regnier F. Structure specific chromatographic selection in targeted proteomics. *J Chromatogr B* 2005; **817**: 23–34
- [5] Tighe P. J, Ryder R. R, Todd I, Fairclough L.C. ELISA in the multiplex era: Potentials and pitfalls. *Proteomics Clin Appl* 2015; **9**: 406–422
- [6] Zhang S, Garcia-D'Angeli A, Brennan J. P, Huo Q. Predicting detection limits of enzyme-linked immunosorbent assay (ELISA) and bioanalytical techniques in general. *Analyst* 2014; **139**: 439-445
- [7] Seger C. Usage and limitations of liquid chromatography-tandem mass spectrometry (LC–MS/MS) in clinical routine laboratories. *Wien Med Wochenschr* 2012; **162**:499–504
- [8] Guan F, Uboh C. E, Soma L. R, Birks E, Chen J, You Y, Rudy J, Li X. Differentiation and identification of recombinant human erythropoietin and darbepoetin Alfa in equine plasma by LC-MS/MS for doping control. *Anal Chem* 2008; **80**: 3811-3817.

- [9] Groleau P. E, Desharnais P, Cote L, Ayotte C. Low LC–MS/MS detection of glycopeptides released from pmol levels of recombinant erythropoietin using nanoflow HPLC–chip electrospray ionization. *J Mass Spectrom* 2008; **43**:924-935.
- [10] Thermo Scientific Pierce Assay Development Technical Handbook, version 2, <https://tools.lifetechnologies.com/content/sfs/brochures/1602127-Assay-Development-Handbook.pdf>
- [11] Han X. X, Zhao B, Ozaki Y. Surface-enhanced Raman scattering for protein detection. *Anal Bioanal Chem* 2009; **394**:1719-1727
- [12] Hering K, Cialla D, Ackermann K, Dörfer T, Möller R, Schneidewind H, Mattheis R, Fritzsche W, Rösch P, Popp J. SERS: a versatile tool in chemical and biochemical diagnostics. *Anal Bioanal Chem* 2008; **390**: 113-124
- [13] Sivanesan A, Ly H. K, Kozuch J, Sezer M, Kuhlmann U, Fischer A, et al. Functionalized Ag nanoparticles with tuneable optical properties for selective protein analysis. *Chem Commun* 2011; **47**: 3553–3555
- [14] Campion A, Kambhupati P. Surface enhanced Raman scattering. *Chem Soc Rev* 1998; **27**: 241-250
- [15] Haynes C. L, McFarland A. D, Van Duyne R. P. Surface enhanced Raman spectroscopy. *Anal Chem* 2005; **77**: 338A-346A
- [16] Qi J, Motwani P, Gheewala M, Brennan C, Wolfe J. C, Shih W. C. Surface-enhanced Raman spectroscopy with monolithic nanoporous gold disk substrates. *Nanoscale* 2013; **5**: 4105-4109

- [17] Nie S, Emory S. R. Probing single molecules and single nanoparticles by surface enhanced Raman scattering. *Science* 1997; **275**: 1102-1106
- [18] Podstawka E, Ozaki Y, Proniewicz L.M. Part III: surface-enhanced Raman scattering of amino acids and their homo dipeptide monolayers deposited onto colloidal gold surface. *Appl Spectrosc* 2005; **59**:1516–1526, 2005
- [19] Xu L. J, Zong C, Zheng X. S, Hu P, Feng J. M, Ren B. Label-free detection of native proteins by surface-enhanced Raman spectroscopy using iodide-modified nanoparticles. *Anal Chem* 2014; **86**: 2238–2245
- [20] Bantz K. C, Meyer A. F, Wittenberg N. J, Im H, Kurtulus Ö, Lee S H, et al. Recent progress in SERS biosensing. *Phys Chem Chem Phys* 2011; **13**: 11551–11567
- [21] Hughes J, Izake E. L, Lott W. B, Ayoko G. A, Sillence M. Ultrasensitive label free surface enhanced Raman spectroscopy method for the detection of biomolecules. *Talanta* 2014; **130**: 20–25
- [22] Sivanesan A, Izake E. L, Agoston R, Ayoko G. A, Sillence M. Reproducible and label free biosensor for the selective extraction and rapid detection of proteins in biological fluids. *J Nanobiotechnol* 2015; **13**: DOI 10.1186/s12951-015-0102-8
- [23] Jelkmann W. Regulation of erythropoietin production. *J Physiol* 2011; **589**: 1251–1258
- [24] Lamon S, Robinson N, Saugy M. Procedures for monitoring recombinant erythropoietin and analogs in doping. *Endocrinol Metab Clin North Am* 2010; **39**:141–154
- [25] Morkeberg J, Lundby C, Nissen-Lie G.R.O, Nielsen T.K, Hemmersbach P, Damsgaard R. Detection of Darbepoetin Alfa Misuse in Urine and Blood: A Preliminary Investigation. *Med Sci Sports Exerc* 2007; **39**, 1742-1747

- [26] Nissen-Lie G.R.O, Birkeland K, Hemmersbach P, Skibeli V. Serum sTfR Levels May Indicate Charge Profiling of Urinary r-hEPO in Doping Control. *Med Sci Sports Exerc* 2004; **36**: 588-593
- [27] Ashenden M, Varlet-Marie E, Lasne F, Audran M. The effects of microdose recombinant human erythropoietin regimens in athletes. *Haematologica* 2006; **91**: 1143-1144
- [28] WADA Technical Document–TD2014EPO.  
<https://wada-main-prod.s3.amazonaws.com/resources/files/WADA-TD2014EPO-v1-Harmonization-of-Analysis-and-Reporting-of-ESAs-by-Electrophoretic-Techniques-EN.pdf>
- [29] Schumacher Y. O, Saugy M, Pottgiesser T, Robinson N. Detection of EPO doping and blood doping: the haematological module of the Athlete Biological Passport. *Drug Test Analysis* 2012; **4**:846–853
- [30] Ciallaa D, Polloka S, Steinbrücker C, Weber K, Popp J. SERS-based detection of biomolecules. *Nanophotonics* 2014; **3**: 383–411
- [31] Bao F, Yao J. L, Gu R. A. Synthesis of Magnetic Fe<sub>2</sub>O<sub>3</sub>/Au Core/Shell Nanoparticles for Bioseparation and Immunoassay Based on Surface-Enhanced Raman Spectroscopy. *Langmuir* 2009; **25**: 10782-10787
- [32] Jain P. K, Xiao Y, Walsworth R, Cohen A. E. Surface plasmon resonance enhanced magneto (SuPREMO): Faraday rotation enhancement in gold-coated iron oxide nanocrystals, *Nano Lett* 2009; **4**: 1644-1650
- [33] Tamer U, Gündoğdu Y, Boyacı İ. H., Kadir Pekmez, Synthesis of magnetic core–shell Fe<sub>3</sub>O<sub>4</sub>–Au nanoparticle for biomolecule immobilization and detection. *J Nanopart Res* 2010; **12**: 1187–1196

- [34] Sharma A, Matharu Z, Sumana G, Solanki P. R, Kim C. G, Malhotra B. D. Antibody immobilized cysteamine functionalized-gold nanoparticles for aflatoxin detection. *Thin Solid Films* 2010; **519**: 1213-1218
- [35] T. Yannick, Brioude A, Coleman A. W, Rhimi M, Kim B. Molecular recognition by gold, silver and copper nanoparticles. *World J Biol Chem* 2013; **4**: 35-63
- [36] Wang W, Wei Q, Wang J, Wang B, Zhang S, Yuan Z. Role of thiol-containing polyethylene glycol (thiol-PEG) in the modification process of gold nanoparticles (AuNPs): Stabilizer or coagulant. *J Colloid Interface Sci* 2013; **404**: 223–229
- [37] Lönnberg M, Dehnes Y, Drevin M, Garle M, Lamon S, Leuenberger N. Rapid affinity purification of erythropoietin from biological samples using disposable monoliths. *J Chromatogr A* 2010; **1217**:7031-7037
- [38] Schmidt M. S, Hübner J, Boisen A. Large Area Fabrication of Leaning Silicon Nanopillars for Surface Enhanced Raman Spectroscopy. *Adv Mater* 2012; **24**: OP11–OP18
- [39] Yang J, Palla M, Bosco F. G, Rindzevicius T, Alstrøm T. S, Schmidt M. S, et al. Surface-enhanced Raman spectroscopy based quantitative bioassay on aptamer-functionalized nanopillars using large-area Raman mapping. *ACS Nano* 2013; **7**: 5350–5359
- [40] Human Erythropoietin Quantikine IVD ELISA Kit.  
<http://www.rndsystems.com/Products/DEP00>
- [41] High quality Raman data for nonhomogeneous samples using Raster Orbital Scanning.  
<http://oceanoptics.com/wp-content/uploads/App-Note-High-Quality-Raman-Data-for-Non-Homogeneous-Samples-Using-Raster-Orbital-Scanning.pdf>



- [42] Hoskins C, Min Y, Gueorguieva M, McDougall C, Volovick A, Prentice P, Wang Z, Melzer A, Cuschieri A, Wang Lijun. Hybrid gold-iron oxide nanoparticles as a multifunctional platform for biomedical application. *J Nanobiotechnol* 2012; **10**: DOI: 10.1186/1477-3155-10-27
- [43] Li Z, Wei L, Gao M. Y, Lei H. One pot reaction to synthesize biocompatible magnetite nanoparticles. *Adv Mater* 2005; **17**: 1001-1005
- [44] Tiwari P. M, Vig K, Dennis V. A, Singh S. R. Functionalized gold nanoparticles and their biomedical applications. *Nanomaterials* 2011; **1**: 31-63
- [45] Gupta A. K, Gupta M. Synthesis and surface engineering of iron oxide nanoparticles for biomedical applications. *Biomaterials* 2005; **26**: 3995-4021
- [46] Drbohlavova J, Hrdy R, Adam V, Kizek R, Schneeweiss O, Hubalek J. Preparation and properties of various magnetic nanoparticles. *Sensors* 2009; **9**:2352-2362
- [47] Rodrigues D. C, Souza M. L, Souza K. S, Dos Santos D. P, Andrade G. F. S, Temperini M. L. A. Critical assessment of enhancement factor measurements in surface-enhanced Raman scattering on different substrates. *Phys Chem Chem Phys* 2015; DOI: 10.1039/C4CP05080K
- [48] Hoskins C, Min Y, Gueorguieva M, McDougall C, Volovick A, Prentice P, et al. Hybrid gold-iron oxide nanoparticles as a multifunctional platform for biomedical application, *J Nanobiotechnol* 2012; **10**: Doi:10.1186/1477-3155-10-27
- [49] Arniza K.M. Jamil, Emad L. Izake, Arumugam Sivanesan, Peter M Fredericks. Rapid detection of TNT in aqueous media by selective label free surface enhanced Raman spectroscopy, *Talanta*, 2005, 134, 732–738.

- [50] Arniza K.M. Jamil, Emad L. Izake, Arumugam Sivanesan, Agoston R, Ayoko G. A. A homogeneous surface-enhanced Raman scattering platform for ultra-trace detection of trinitrotoluene in the environment. *Anal Methods* 2015; **7**: 3863-3868
- [51] Podstawka E, Ozaki Y, Proniewicz L. M. Adsorption of S–S Containing Proteins on a Colloidal Silver Surface Studied by Surface-Enhanced Raman Spectroscopy. *Appl Spectrosc* 2004; **58**: 1147-1156
- [52] Kahraman M, Wachsmann-Hogiu S. Label-free and direct protein detection on 3D plasmonic nanovoid structures using surface-enhanced Raman scattering. *Anal Chim Acta* 2015; **856**: 74-81
- [53] Kumar G. V. P, Selvi R, Kishore H. A, Kundu T. K, Narayana C. Surface-Enhanced Raman spectroscopic studies of coactivator-associated arginine methyltransferase 1. *J Phys Chem B* 2008; **112**: 6703-6707
- [54] Wang J, Lin D, Lin J, Yu Y, Huang Z, Chen Y, et al. Label-free detection of serum proteins using surface-enhanced Raman spectroscopy for colorectal cancer screening. *J Biomed Opt* 2014; **DOI**: 10.1117/1.JBO.19.8.087003.
- [55] Yang X, Gu C, Qian F, Li Y, Zhang J. Z. Highly sensitive detection of proteins and bacteria in aqueous solution using surface-enhanced Raman scattering and optical fibres. *Anal Chem* 2011; **83**: 5888-5894
- [56] Wang M, Benford M, Jing N, Coté G, Kameoka J. Optofluidic device for ultra-sensitive detection of proteins using surface-enhanced Raman spectroscopy. *Microfluid Nanofluid* 2009; **6**: 411-417

[57] Kundu P. P, Bhowmick T, Swapna G, Kumar G. V. P, Nagaraja V, Narayana C. Allosteric transition induced by  $Mg^{2+}$  ion in a transactivator monitored by SERS. *J Phys Chem B* 2014; **118**: 5322-5330

[58] Pagba C. V, Lane S. M, Cho H, Wachsmann-Hogiu S. Direct detection of aptamer-thrombin binding via surface enhanced Raman spectroscopy. *J Biomed Opt* 2010; **DOI**: 10.1117/1.3465594

[59] Aachmann-Andersen N. J, Christensen S. J, Lisbjerg K, Oturai P, Meinild-Lundby A, Holstein-Rathlou N, et al. Recombinant erythropoietin in humans has a prolonged effect on circulating erythropoietin isoform distribution, *PLoS One* 2014; **DOI**: 10.1371/journal.pone.0110903

[60] Kurouski D, Van Duyne R. P. In situ detection and identification of hair dyes using surface enhanced Raman spectroscopy (SERS), *Anal Chem* 2015; **87**: 2901-2906.

**Figure legends**

Figure 1, TEM and histograms of a) iron oxide nanoparticles and b) magnetic core gold nanoparticles

Figure 2, XRD of iron oxide nanoparticles

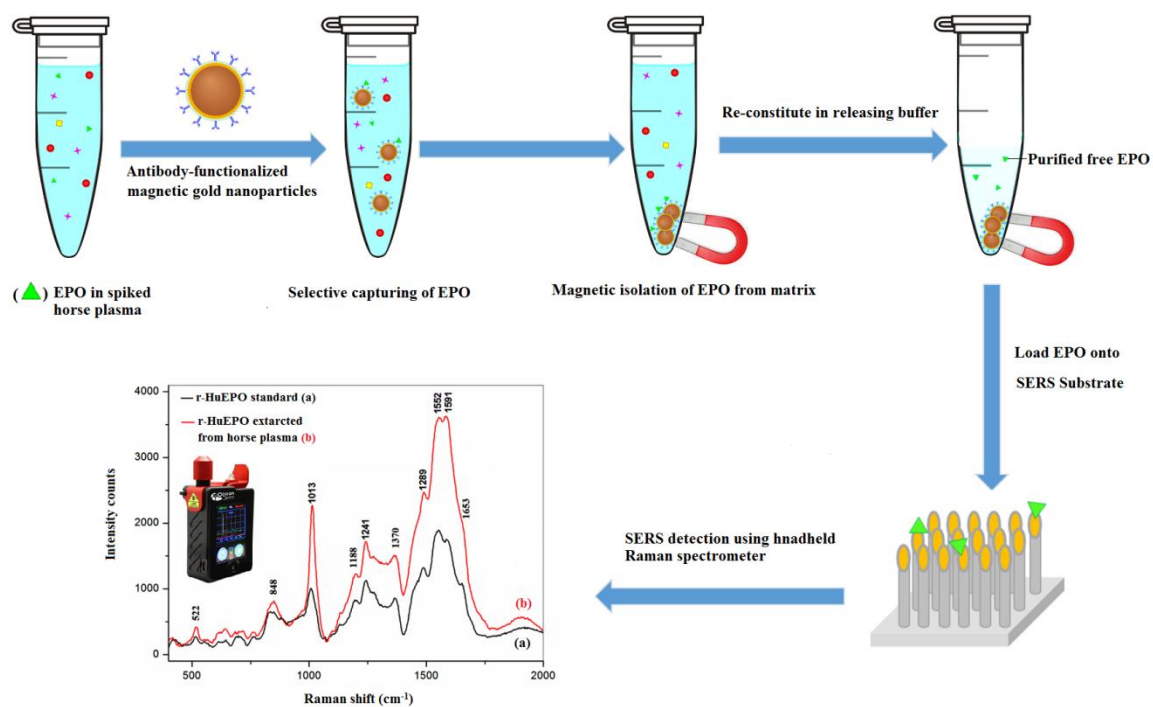
Figure 3: UV-Vis absorption spectrum of magnetic core gold nanoparticles

Figure 4: SERS spectrum of antibody-functionalized gold nanoparticles a) before and b) after binding with rHuEPO

Figure 5: SERS spectrum of a) rHuEPO standard and b) rHuEPO extracted from horse plasma. Measurements were carried out on old-coated silicon nanopillars SERS substrate and using the inVia Renishaw Raman spectrometer.

Figure 6: SERS spectrum of a) rHuEPO standard and b) rHuEPO extracted from horse plasma. Measurements were carried out on using handheld Raman spectrometer (1 minute measurement time per sample). Spectra were collected using 785 nm excitation wavelength and a single 40 second accumulation in the Raster Orbital Scanning (ROS) mode

Figure 7: a) SERS spectra, at  $1551\text{ cm}^{-1}$ , of rHuEPO in the concentration range 50 nM to 5 pM and b) Plot demonstrating the linear relationship between log concentration of rHuEPO and SERS intensity at  $1551\text{ cm}^{-1}$



## Graphical Abstract

Schematic diagram of the selective protein isolation and detection by magnetic nanoparticles and portable Raman spectroscopy

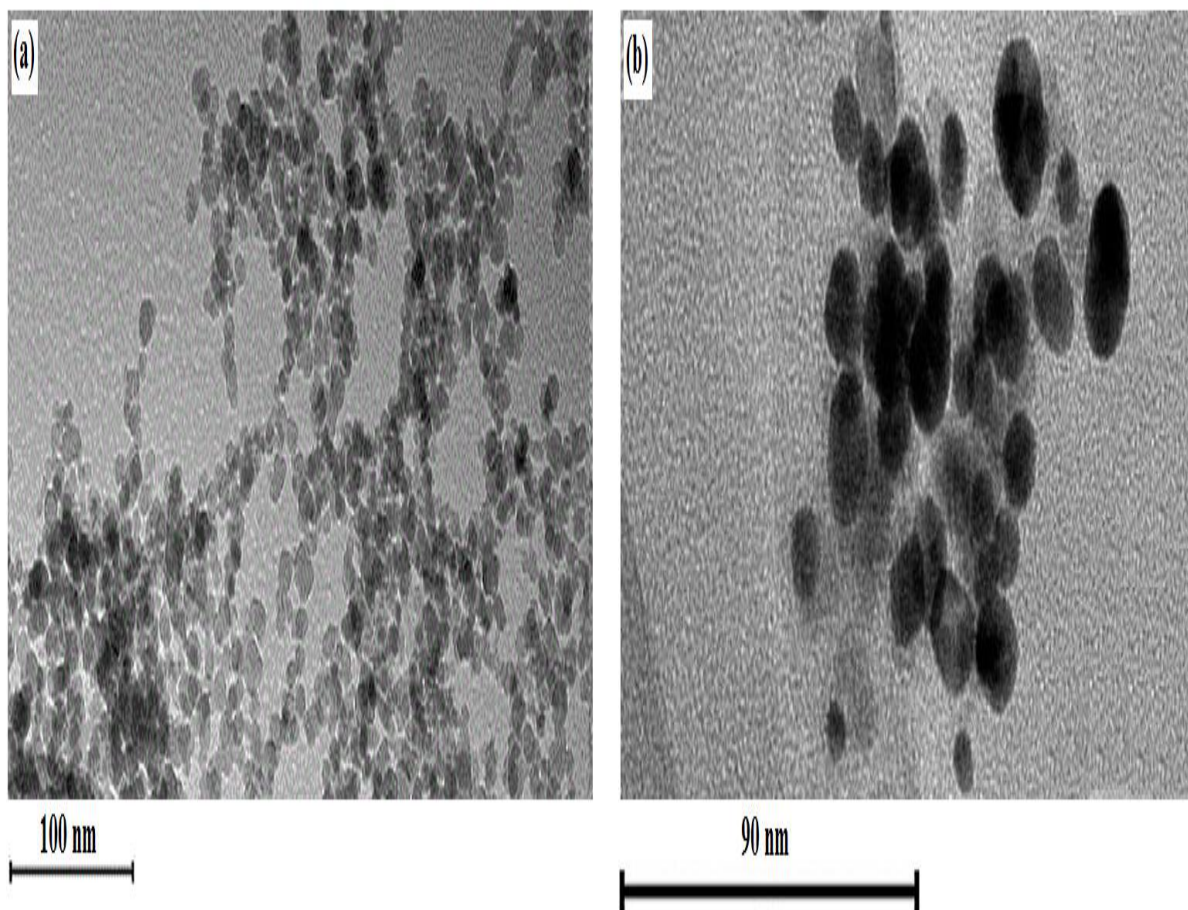


Figure 1

ACCEPTED

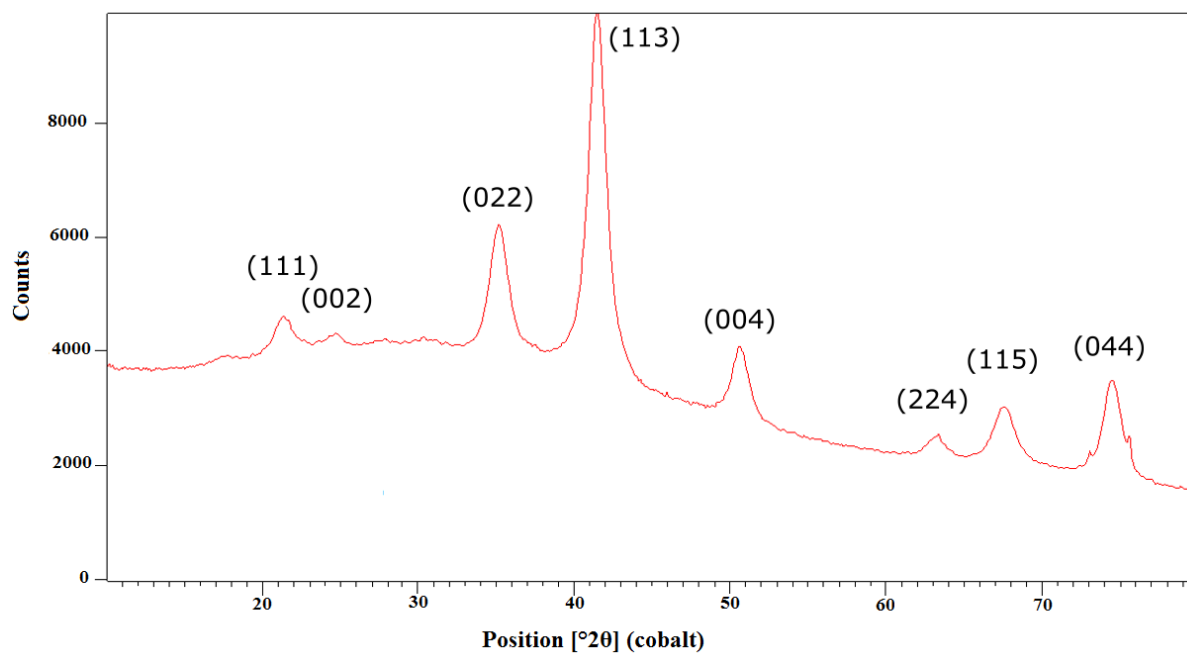


Figure 2

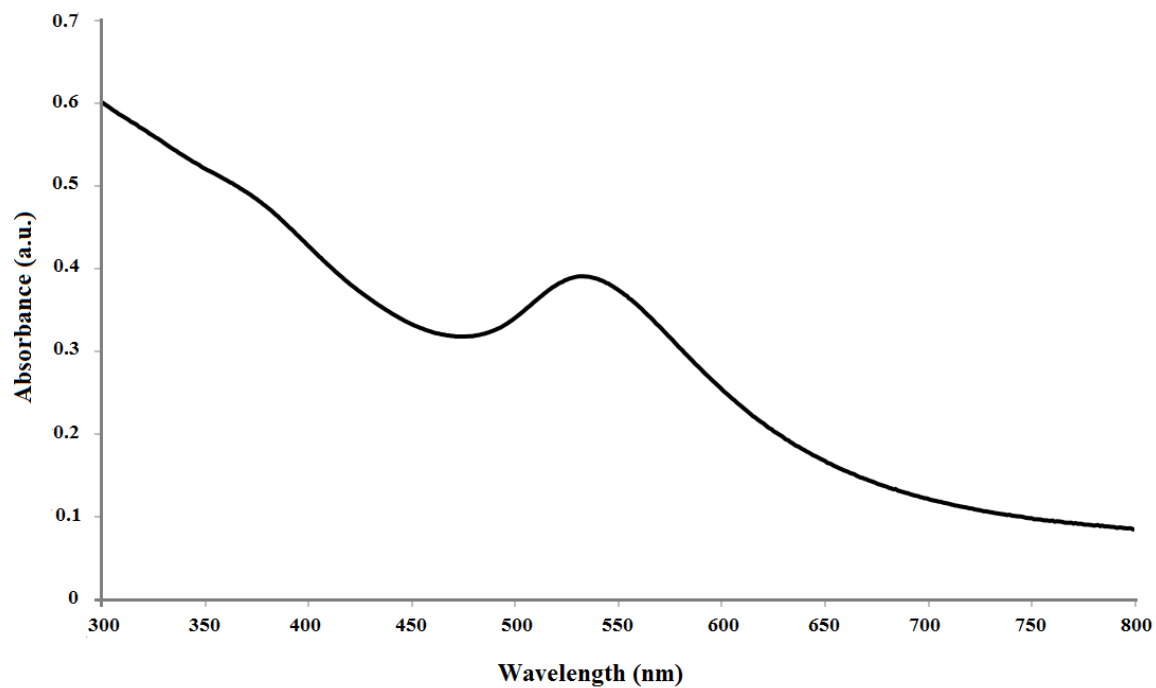


Figure 3

ACCEPTED



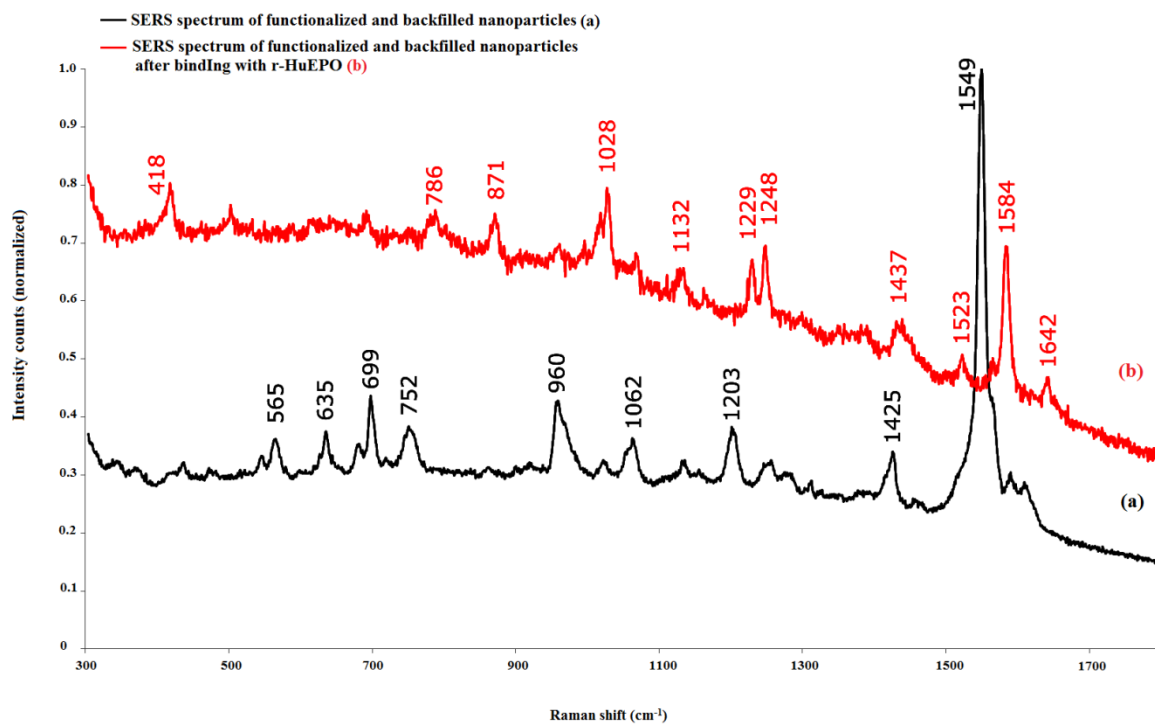


Figure 4

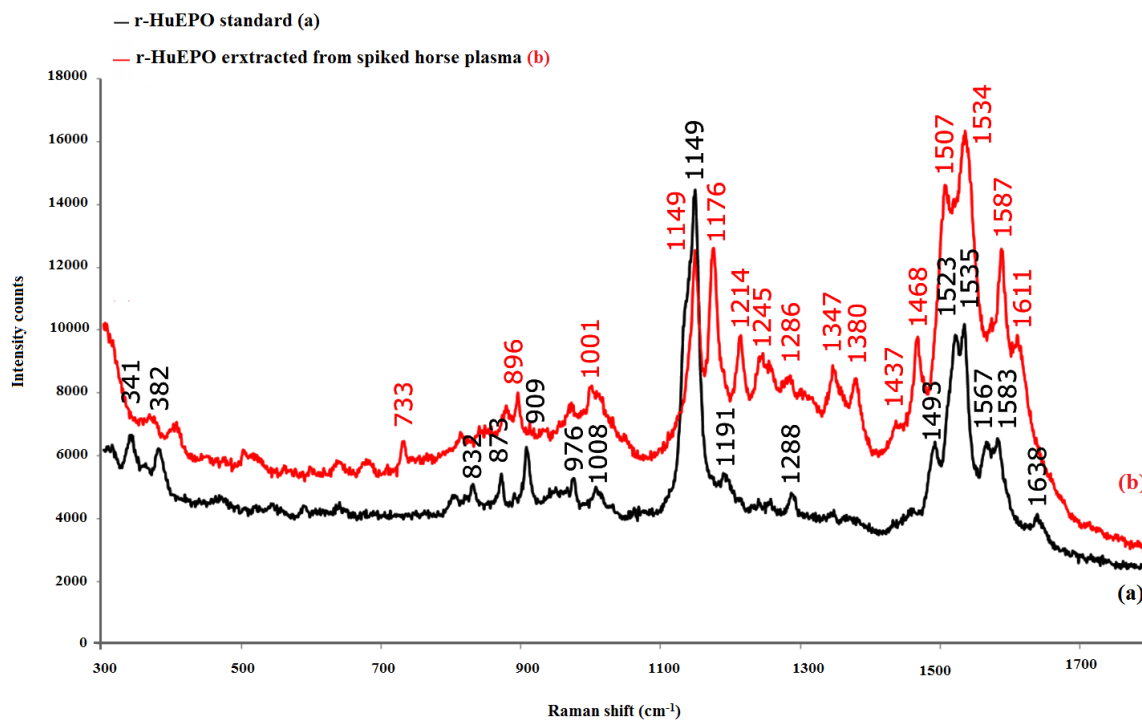


Figure 5

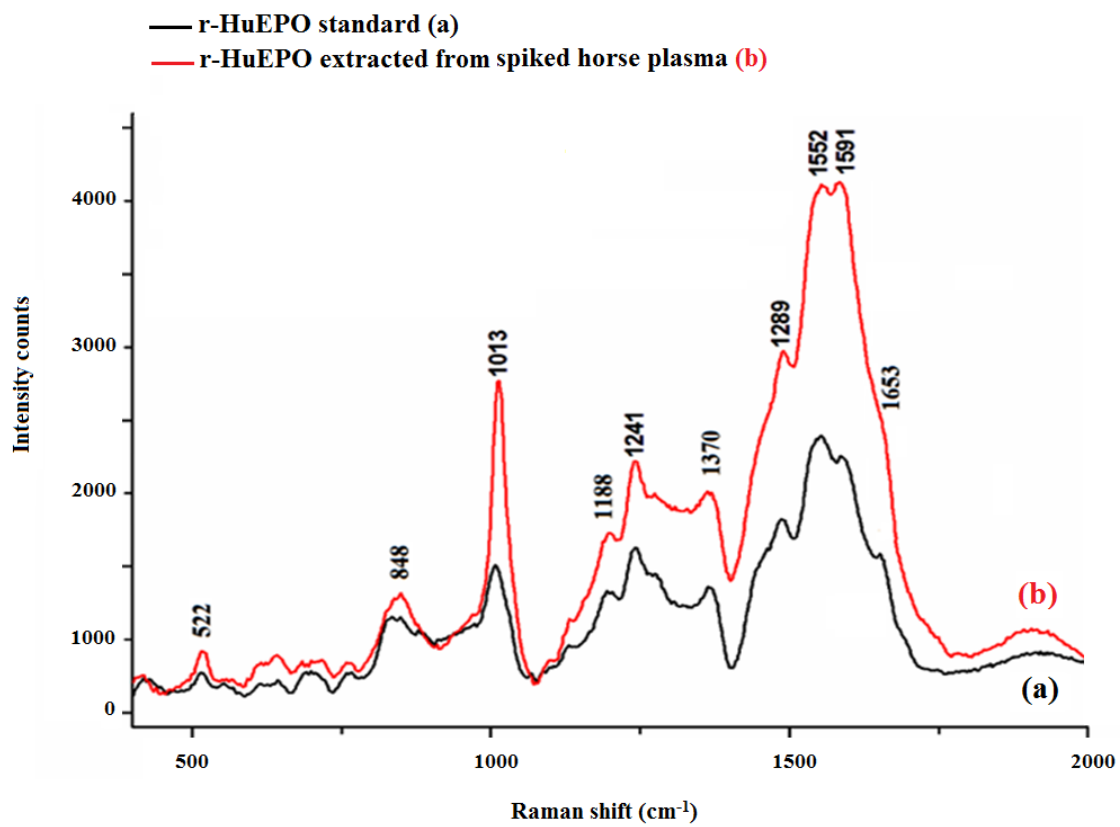


Figure 6

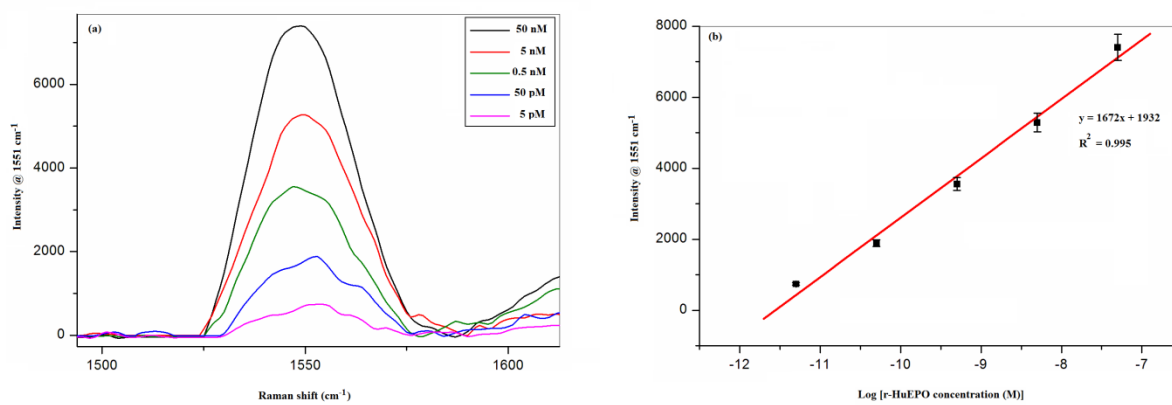


Figure 7

Table 1, assignments of Raman bands in the SERS Spectra (Fig 5b) of r-HuEPO extracted from spiked horse plasma

Raman shift (cm <sup>-1</sup> )	Band assignment	Reference
1001	Benzene ring breathing of phenylalanine	52
1149	ring stretch / $\nu_{as}(C_{\alpha}CN)$	53, 57
1176	Phenylalanine, Tyrosine	51, 55, 56
1214	Phenylalanine	51, 58
1245	Amide III	51, 57
1286	Amide III	51
1347	Tryptophan	51, 57
1380	$\nu_{as}(COO^-)$	51, 53
1468	CH <sub>2</sub> (scissoring)	52, 53, 57
1507	Phenylalanine, Histidine, Tryptophan	51, 55
1534	Amide II	53
1587	Tryptophan, Tyrosine, Phenylalanine	53, 56, 58
1611	Amide I ( $\alpha$ helix), Phenylalanine	51, 52, 57